Homogenization and mixing measures for a replenishing passive scalar field

Shane R. Keating,[1] Peter R. Kramer,[2] and K. Shafer Smith[1]
[1]*Center for Atmosphere-Ocean Science, Courant Institute of Mathematical Sciences, New York University, 251 Mercer Street, New York, New York 10012, USA*
[2]*Department of Mathematical Sciences, Rensselaer Polytechnic Institute, Troy, New York 12180, USA*

(Received 31 October 2009; accepted 25 May 2010; published online 16 July 2010)

The efficiency with which an incompressible flow mixes a passive scalar field that is continuously replenished by a steady source-sink distribution has been quantified using the suppression of the mean scalar variance below the value it would attain in the absence of the stirring. We examine the relationship this mixing measure has to the effective diffusivity obtained from homogenization theory, particularly establishing precise connections in the case of a stirring velocity field that is periodic in space and time and varies on scales much smaller than that of the source. We explore theoretically and numerically via the Childress–Soward family of flows how the mixing measures lose their linkage to the homogenized diffusivity when the velocity and source field do not enjoy scale separation. Some implications for homogenization-based parametrizations of mixing by flows with finite scale separation are discussed. © *2010 American Institute of Physics*.
[doi:10.1063/1.3456726]

I. INTRODUCTION

Mixing phenomena are the object of active and ubiquitous study in physics, engineering and the geosciences, and a major branch of fluid-dynamical research is concerned with the archetypal mixing problem: that of passively advected scalar fields in turbulent and chaotic flows.[1–8] Characterizing the relevant mixing properties of a flow is a highly contextual exercise, but a great deal of insight can be gained from the study of fluctuations of a passively advected scalar field injected into the flow. For example: mixing in microfluidic devices,[9] anthropogenic and controlled-release tracers in the ocean,[10] observed temperature, chlorophyll and biogeochemical distributions,[11] or offline advection of "virtual" tracers.[12]

When a passive scalar field $\theta(\boldsymbol{x},t)$ is continually replenished by a temporally steady, spatially inhomogeneous distribution of sources and sinks, the variance of the fluctuations in the scalar field can attain a statistically steady balance between injection and dissipation. Doering and Thiffeault[13] propose a natural mixing diagnostic using such a replenishing passive scalar field: the *mixing efficiency* of the flow is defined as the suppression of the equilibrium variance of the scalar field $\langle\theta^2\rangle$ below the value it would attain in the *absence* of the stirring field $\langle\theta_0^2\rangle$,

$$E_0 := \sqrt{\frac{\langle\theta_0^2\rangle}{\langle\theta^2\rangle}}, \tag{1a}$$

where angle brackets denote spatiotemporal averaging and mean stirred and unstirred tracer concentrations are assumed to be zero. Information about mixing on small and large scales is obtained in a similar way by weighting the sums of the Fourier components of the stirred and unstirred scalar fields to microscales and macroscales, respectively, viz.,

$$E_{+1}^2 := \frac{\langle|\boldsymbol{\nabla}\theta_0|^2\rangle}{\langle|\boldsymbol{\nabla}\theta|^2\rangle} = \frac{\Sigma_{\boldsymbol{k}} k^2|\hat{\theta}_{0\boldsymbol{k}}|^2}{\Sigma_{\boldsymbol{k}} k^2|\hat{\theta}_{\boldsymbol{k}}|^2}, \tag{1b}$$

$$E_{-1}^2 := \frac{\langle|\boldsymbol{\nabla}^{-1}\theta_0|^2\rangle}{\langle|\boldsymbol{\nabla}^{-1}\theta|^2\rangle} = \frac{\Sigma_{\boldsymbol{k}} k^{-2}|\hat{\theta}_{0\boldsymbol{k}}|^2}{\Sigma_{\boldsymbol{k}} k^{-2}|\hat{\theta}_{\boldsymbol{k}}|^2}, \tag{1c}$$

with $|\boldsymbol{k}|^2=k^2$. The Fourier series of a function $g(\boldsymbol{x})$ with period L in each of d spatial dimensions is given by

$$g(\boldsymbol{x}) = \sum_{\boldsymbol{k}\in\mathbb{Z}^d} \hat{g}_{\boldsymbol{k}} e^{i\boldsymbol{k}\cdot\boldsymbol{x}/L}, \quad \hat{g}_{\boldsymbol{k}} = \frac{1}{L^d}\int_{[0,L]^d} g(\boldsymbol{x}) e^{-i\boldsymbol{k}\cdot\boldsymbol{x}/L} d\boldsymbol{x}, \tag{2}$$

so that the "antigradient" operator $\boldsymbol{\nabla}^{-1}$ has, in a periodic domain, the unambiguous interpretation as the Fourier transform of the vector $-iL\boldsymbol{k}/k^2$. Another multiscale mixing measure which can be shown to be equal to similar fractional Sobolev norms has been developed by Mathew *et al.*[9,14]

Part of the power of the multiscale mixing efficiency formulation lies in its amenability to rigorous analysis in terms of upper and lower bounds and the asymptotic dependence of these bounds on the shape of the source function and the strength of the stirring field, the latter being quantified by the Péclet number,

$$\mathrm{Pe} := \frac{U\ell}{\kappa}, \tag{3}$$

where U and ℓ are the velocity and length scale of the energy-containing eddies. Under the condition that the velocity field is incompressible and the scale separation δ between the source and the stirring fields is a fixed finite quantity, Thiffeault *et al.*[15] and Doering and Thiffeault[13] obtained upper and lower bounds for the multiscale mixing efficiencies. For large Péclet number, these bounds scale as

$$A^- \leq E_p \leq A^+ \mathrm{Pe}^{\alpha}, \tag{4}$$

where the exponent $0 \leq \alpha \leq 1$ depends on the shape of the source. For each p, the A^- are $O(1)$ coefficients and A^+ is a function of the scale separation. These bounds are sharp in the sense that they are very nearly saturated for certain source-flow combinations.[16,17]

A natural question is how the mixing measures are related to the effective diffusivity obtained in homogenization theory.[2,18–22] Lin *et al.*[23] clarified this through a detailed examination of a stirring field with a shear flow structure, showing that the mixing efficiencies (for $p=0$ and $p=-1$) and homogenized effective diffusivity have the same scaling with respect to Pe when the ratio δ of the scale of the stirring velocity field to that of the source/sink field is sufficiently strong so that $\delta \ll \mathrm{Pe}^{-1}$. When $\delta \gtrsim \mathrm{Pe}^{-1}$, the mixing measures are in general found to be distinct from that of homogenization theory and to scale differently with respect to Péclet number. The bounds (4) on the mixing measures only apply to the case where the stirring and source/sink fields have the same length scales; Lin *et al.*[23] generalize this bound to the case of arbitrary scale separation and show that the effective diffusivity of homogenization theory satisfies these modified bounds.

Here we complement the findings of Lin *et al.*[23] by approaching the question from the general homogenization framework rather than a detailed study of a particular example. We will establish in Sec. II the general connection between the mixing measures and homogenization theory when the scale separation condition $\delta \ll \mathrm{Pe}^{-1}$ is satisfied. In Sec. III, we illustrate the behavior and relationship of homogenized effective diffusivity and mixing measures numerically on the Childress–Soward class of flows, which comprises examples with a wide range of mixing effectiveness. Finally, we offer some concluding remarks and practical implications for homogenization-based parametrizations of mixing in Sec. IV.

II. RELATIONSHIP BETWEEN MULTISCALE MIXING EFFICIENCIES AND HOMOGENIZED DIFFUSIVITY IN FLOWS WITH SCALE SEPARATION

Consider a passive scalar field $\theta(\boldsymbol{x},t)$ evolving as

$$\frac{\partial \theta}{\partial t} + \mathcal{L}\theta = s(\boldsymbol{x}), \quad \mathcal{L} = \boldsymbol{v} \cdot \boldsymbol{\nabla} - \kappa\Delta, \tag{5}$$

where $s(\boldsymbol{x})$ is a steady source/sink term, $\boldsymbol{v}(\boldsymbol{x},t)$ is an incompressible stirring velocity field, and κ the molecular diffusivity. We restrict attention here to steady sources for the sake of simplicity; however, much of our discussion carries over to the case of a time-dependent source.[18] For brevity, we will simply refer to $s(\boldsymbol{x})$ as the source field, understanding that negative values of s correspond to sinks of the passive scalar field. Both the source and stirring fields will be assumed to be periodic in space with period lengths L and ℓ along each Cartesian direction, respectively, and the velocity field will be assumed to be periodic in time with period τ, although the same formal arguments apply for the case where the source and stirring fields are homogeneous and stationary random fields with these length and time scales associated with finite correlation lengths.[18,19,24–28] The unstirred field $\theta_0(\boldsymbol{x},t)$ is the solution to the analogous, unstirred diffusion equation, with the same diffusivity and source,

$$\frac{\partial \theta_0}{\partial t} + \mathcal{L}_0\theta_0 = s(\boldsymbol{x}), \quad \mathcal{L}_0 = -\kappa\Delta. \tag{6}$$

We will assume the spatial average of the source is zero, so that it does not drive an indefinite growth in the passive scalar field. One can straightforwardly show that in this case the passive scalar field itself will also settle into a zero spatial average state,

$$\langle s \rangle = 0 = \langle \theta \rangle. \tag{7}$$

As is well-known, the gross effect of the stirring field can be parametrized in terms of an effective diffusivity tensor on length scales large compared to that of the stirring ℓ. In particular, when the length scale of the source is large compared to that of the velocity field ($\delta \equiv \ell/L \ll 1$), the advection-diffusion operator in Eq. (5) can be replaced by an effective diffusion operator,[18]

$$\frac{\partial \theta}{\partial t} + \mathcal{L}^*\theta = s(\boldsymbol{x}) + O(\delta), \quad \mathcal{L}^* = -\sum_{i,j=1}^{d} D_{ij}\frac{\partial}{\partial x_i}\frac{\partial}{\partial x_j}. \tag{8}$$

The effective diffusivity tensor D_{ij} represents, in terms of a bulk diffusivity, the effect of the rapidly evolving stirring field on the large-scale evolution of the passive scalar field, and can be expressed as

$$D_{ij} = \kappa(\delta_{ij} + \bar{K}_{ij}), \tag{9}$$

where $\bar{K}_{ij}$ is the enhancement of the diffusivity above its isotropic molecular value κ.

Homogenization theory provides a rigorous framework within which the coefficients of the effective diffusivity tensor can be calculated exactly in the limit of asymptotically strong scale-separation $\delta \ll 1$.[2,18–22] Concretely, the effective diffusivity tensor is expressed in terms of the solution to an associated cell problem involving functions of the small-scale variables alone. The small-scale velocity field is then said to be "homogenized" over its periodic cell, and its effect upon the passively advected scalar field appears as an enhancement of the bare, molecular diffusivity.

We note that homogenization theory is usually formulated in the context of *freely evolving* passive scalar turbulence, and that the presence of a small-scale component of the source can introduce some nontrivial coupling with the small-scale velocity field that can give rise to an effective large-scale production of scalar concentration.[18] However, the homogenization proceeds more straightforwardly for the case described above, where the source field varies on a single length scale L large compared to the single length scale ℓ of variation of the velocity field.

The homogenized diffusion Eq. (8) is linear and can be straightforwardly solved on a periodic domain for each Fourier mode, to give, in the limit $t \to \infty$,

$$\hat{\theta}_{\boldsymbol{k}}(t) = \frac{\hat{s}_{\boldsymbol{k}}}{\Sigma_{i,j=1}^{d} D_{ij} k_i k_j}. \tag{10}$$

The multiscale mixing efficiencies E_0 and E_{-1} can then be calculated as

$$E_{-1}^2 = \frac{\Sigma_{\boldsymbol{k}} |\hat{s}_{\boldsymbol{k}}|^2 / k^6}{\Sigma_{\boldsymbol{k}} |\hat{s}_{\boldsymbol{k}}|^2 / k^2 \left(k^2 + \Sigma_{i,j=1}^{d} \bar{K}_{ij} k_i k_j\right)^2}, \tag{11a}$$

$$E_0^2 = \frac{\Sigma_{\boldsymbol{k}} |\hat{s}_{\boldsymbol{k}}|^2 / k^4}{\Sigma_{\boldsymbol{k}} |\hat{s}_{\boldsymbol{k}}|^2 \Big/ \left(k^2 + \Sigma_{i,j=1}^{d} \bar{K}_{ij} k_i k_j\right)^2}. \tag{11b}$$

The expression for the microscale-weighted mixing efficiency E_{+1} is somewhat different from those given in Eqs. (11a) and (11b) because a naive application of homogenization theory can be shown to be theoretically invalid in describing this microscale-weighted mixing efficiency even at strong scale separation. This may be understood by examining the multiscale expansion in the derivation of homogenization theory,[2,18–22] where one can check that the gradient of the true passive scalar field is approximated, in the strong scale separation limit, by the sum of the gradient of the homogenized passive scalar field and a nontrivial corrector term that is closely connected to the solution of the cell problem (15). A careful examination of homogenization theory (described in the Appendix) shows that the microscale-weighted mixing efficiency should actually take the form

$$E_{+1}^2 = \frac{\Sigma_{\boldsymbol{k}} |\hat{s}_{\boldsymbol{k}}|^2 / k^2}{\Sigma_{\boldsymbol{k}} |\hat{s}_{\boldsymbol{k}}|^2 \Big/ \left(k^2 + \Sigma_{i,j=1}^{d} \bar{K}_{ij} k_i k_j\right)}. \tag{11c}$$

The mixing efficiencies E_p assume a particularly simple form when the source function $s(\boldsymbol{x})$ is monochromatic, with wavenumber $\boldsymbol{k}_s$, say. In that case, the spectral sums in Eqs. (11a)–(11c) are easily carried out and the mixing efficiencies reduce to

$$E_0 = E_{-1} = \frac{\Sigma_{i,j=1}^{d} D_{ij} \hat{n}_i \hat{n}_j}{\kappa}, \quad E_{+1} = \sqrt{\frac{\Sigma_{i,j=1}^{d} D_{ij} \hat{n}_i \hat{n}_j}{\kappa}}, \tag{12}$$

where $\hat{\boldsymbol{n}}$ is the unit vector directed along $\boldsymbol{k}_s$. Notice that when the source is monochromatic the macroscale-weighted and unweighted mixing efficiencies E_{-1} and E_0 take the same value, equal to the *square* of the microscale-weighted mixing efficiency E_{+1}. Equation (12) relates the mixing efficiencies directly to the component of the effective diffusivity tensor aligned with the source field. Thus, we see that, for this special combination of a monochromatic source with a small-scale flow, the mixing efficiencies and the effective diffusivity tensor are related in a simple and intuitive manner, except that the small-scale mixing efficiency scales as the square root rather than in simple proportion to the effective diffusivity.

For broader spectrum sources, the precise relationship between the mixing efficiencies and the effective diffusivity depends in a nonuniversal way on the detailed spatial structure of the source. We can show, however, that we can expect similar scaling for the mixing measures E_0 and E_{-1} with respect to Péclet number as for the effective diffusivity in the regime $1 \ll \mathrm{Pe} \ll \delta^{-1}$. We note first that the enhanced diffusivity $\bar{K}(\hat{\boldsymbol{n}}) = \Sigma_{i,j=1}^{d} \bar{K}_{ij} \hat{n}_i \hat{n}_j$ obeys the following rigorous bounds from homogenization theory:[25,29,30]

$$0 \le \bar{K}(\hat{\boldsymbol{n}}) \le C^+(\hat{\boldsymbol{n}}) \mathrm{Pe}^2, \tag{13}$$

where $\hat{\boldsymbol{n}}$ is an arbitrary unit vector and $C^+(\hat{\boldsymbol{n}})$ is some bounded function depending on the structure of the velocity field. Moreover, shear flows can be shown to saturate the upper bound along the shearing direction and the lower bound in the cross-shear direction. Intermediate scalings can be achieved by a variety of other flows.[2,31–33] Now, if the flow exhibits minimally enhanced diffusion[25,34] so that $\|\bar{K}\|$ remains bounded with respect to increasing Péclet number, then clearly the mixing efficiencies E_0 and E_{-1} (11c) will also remain bounded. If, on the other hand, $\|\bar{K}\| \sim \mathrm{ord}(\mathrm{Pe}^{\beta})$ with $0 < \beta \le 2$, then a direct asymptotic calculation on Eq. (11) shows that the multiscale mixing efficiencies will generically exhibit the same scaling $E_0, E_{-1} \sim \mathrm{ord}(\mathrm{Pe}^{\beta})$ provided the interval $1 \ll \mathrm{Pe} \ll \delta^{-1}$ is broad enough. By similar reasoning, the microscale-weighted mixing efficiency will exhibit the scalings $E_{+1} \sim \mathrm{ord}(1)$ and $E_{+1} \sim \mathrm{ord}(\mathrm{Pe}^{\beta/2})$ for minimally and maximally diffusive flows, respectively. Now, if the homogenized diffusivity has different scalings with respect to Péclet number along different directions (as most notably illustrated by the shear flow), the multiscale mixing efficiency will reflect the scaling of the homogenized diffusivity along the strongest direction of transport, provided that the source field has nontrivial variation along that direction. The constant prefactor of the scaling in the multiscale mixing measures, though, depends not only on the scaling prefactor in the effective diffusivity but also on the structure of the source term.

III. NUMERICAL SIMULATIONS

We now explore the relationship between the multiscale mixing measures and homogenized diffusivity through numerical simulations of passive scalar advection in the Childress–Soward flow, described by the one-parameter family of streamfunctions[35,36]

$$\psi = \Gamma \left(\sin\frac{x}{\lambda} \sin\frac{y}{\lambda} + \epsilon \cos\frac{x}{\lambda} \cos\frac{y}{\lambda} \right), \tag{14}$$

where $2\pi\lambda$ denotes the period length and Γ is chosen so that the velocity $\boldsymbol{u} = (\partial_y \psi, -\partial_x \psi)$ has a root-mean-square value of unity. This family of steady, two-dimensional flows is a particularly useful one for studying the effect of changes in streamline topology on the transport properties of the flow, as the parameter ϵ can be varied between zero, corresponding to cellular flow, and one, corresponding to a simple shear flow. For values of $0 < \epsilon < 1$ the flow is a combination of cat's-eye vortices and open channels, the width of the vortices decreasing with increasing ϵ. Streamline patterns for various values of ϵ are depicted in Fig. 1.

Despite its relative simplicity, the Childress–Soward flow exhibits several novel features of interest here. In particular, when $\epsilon > 0$ we expect scalar advection to be en-

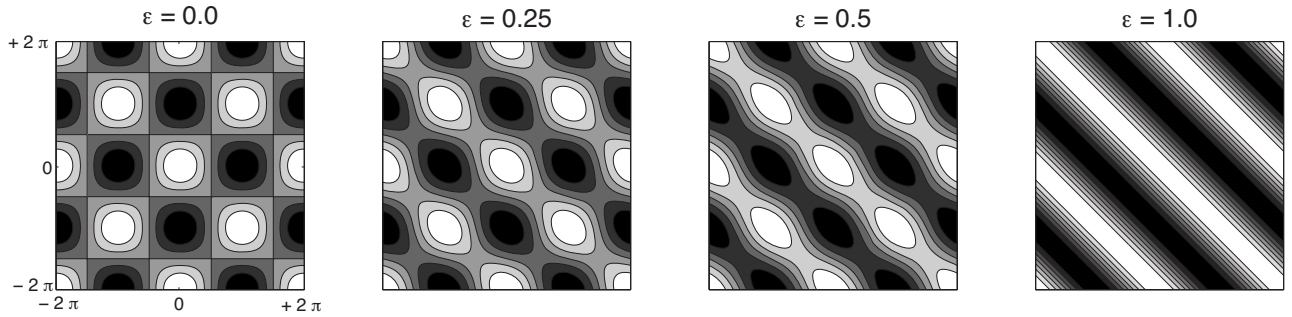

FIG. 1. Sample streamfunctions for the Childress–Soward flow (14) with values of ϵ=0, 0.25, 0.5, and 1.0 and λ=1.

hanced along the direction of the open channels but blocked in the direction orthogonal to the channels. Indeed, the results of detailed analysis[30,35] and numerical computations[34,36] confirm this intuition, showing maximally enhanced diffusion (Pe^2 scaling of the enhanced diffusivity) along open channels and streamline blocking in the orthogonal direction.

Figure 2 plots the Pe-scaling of the diffusivity enhancement $\bar{K}(\hat{\boldsymbol{n}})$ in the along-channel direction $\hat{\boldsymbol{n}}=(\hat{\boldsymbol{x}}-\hat{\boldsymbol{y}})/\sqrt{2}$ for stirring fields with ϵ=0.0, 0.25, 0.5, and 1.0. (A similar figure appears in Majda and McLaughlin.[34]) The values of $\bar{K}(\hat{\boldsymbol{n}})$ were calculated by solving the following cell problem over a spatial period domain of the velocity field on a 128^2 grid,

$$\partial_t \boldsymbol{\chi} + \mathbf{u}\cdot\nabla\boldsymbol{\chi} = \kappa\Delta\boldsymbol{\chi} - \mathbf{u}, \tag{15}$$

with periodic boundary conditions for $\boldsymbol{\chi}$, and then computing the period average

$$\bar{\mathsf{K}} = -\kappa^{-1}\langle \mathbf{u}\otimes\boldsymbol{\chi}\rangle. \tag{16}$$

Only the symmetric part of $\bar{\mathsf{K}}$ contributes to diffusive transport. Note that as the cell problem (15) only involves the single scale of the stirring field it can be solved numerically for moderate Péclet numbers with a relatively low spatial resolution of 128^2 grid points. Direct calculations for the original partial differential Eq. (5) must resolve both the stirring and source field and thus require a commensurately more expensive computation when the scales of these fields are substantially separated.

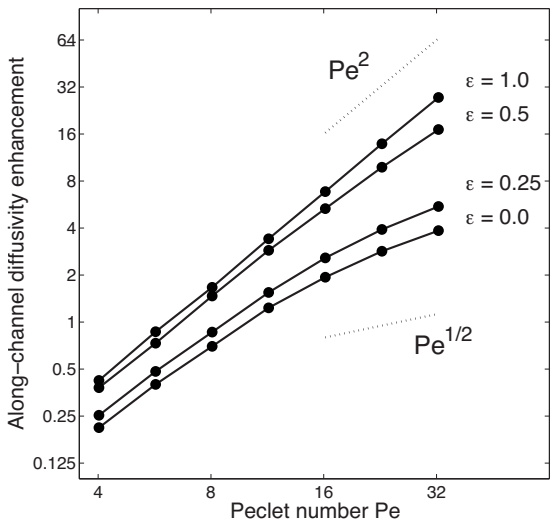

FIG. 2. Log-log plot of the along-channel diffusivity enhancement vs Péclet number for Childress–Soward flows with ϵ=0.0 (cellular flow), 0.25, 0.5, and 1.0 (shear flow). Dotted lines indicate scalings of Pe^2 and $Pe^{1/2}$ for comparison.

A clear Pe^2-scaling is seen for a shear flow (ϵ=1.0), decreasing to a rough $Pe^{1/2}$ scaling for the case of a cellular flow (ϵ=0.0). The physical mechanism underlying the observed Pe^2-scaling is well understood as a consequence of Taylor shear dispersion,[37] whereby particles of tracer are transported coherently and ballistically along streamlines. The effect of molecular diffusion is to randomly kick particles onto neighboring streamlines, leading to rapid decorrelation of particle pairs and a *decrease* in the net tracer transport. As a linear scaling of $\bar{\mathsf{K}}$ with respect to Pe corresponds to an insensitivity of the turbulent diffusivity D (9) with respect to molecular diffusion, we therefore expect and observe a faster-than-linear scaling with respect to Péclet number, and in fact the enhanced diffusivity of the shear flow has the maximal scaling with respect to Péclet number.[2,34] On the other hand, the sublinear $Pe^{1/2}$-scaling for cellular flows is a consequence of trapping within cells, and the need for molecular diffusion to assist in moving the passive scalar field from cell to cell.[2,30,31,34–36]

In computing the multiscale mixing measures (1) for the Childress–Soward flows, we solve the advection-diffusion Eq. (5) with steady source $s(\boldsymbol{x})=\cos(x-y)/L$ varying on the length scale L and oriented orthogonally to the direction of the open channels. We use a pseudospectral code with N=1024 grid points in each of the two dimensions. We present our results nondimensionally in terms of the Péclet number Pe and length scale ratio δ between the variation in the stirring and source fields,

$$\mathrm{Pe}=\frac{\lambda U}{\kappa}, \quad \delta=\frac{\lambda}{L}, \tag{17}$$

where U=1 through our choice of Γ in Eq. (14). As we shall always take δ^{-1} to be an integer, it suffices to solve the advection-diffusion equation over a single period domain of the source (which may contain many periods of the stirring velocity field). Our resolution requirements restrict the range of parameters we can explore as follows: the diffusion scale of the passive scalar field, which we must resolve, can be estimated by $\Delta=(\lambda\kappa/U)^{1/2}$. We therefore require $L/N \lesssim \Delta$. Noting that we can express the Péclet number as $\mathrm{Pe}=(\lambda/\Delta)^2$, we infer the condition

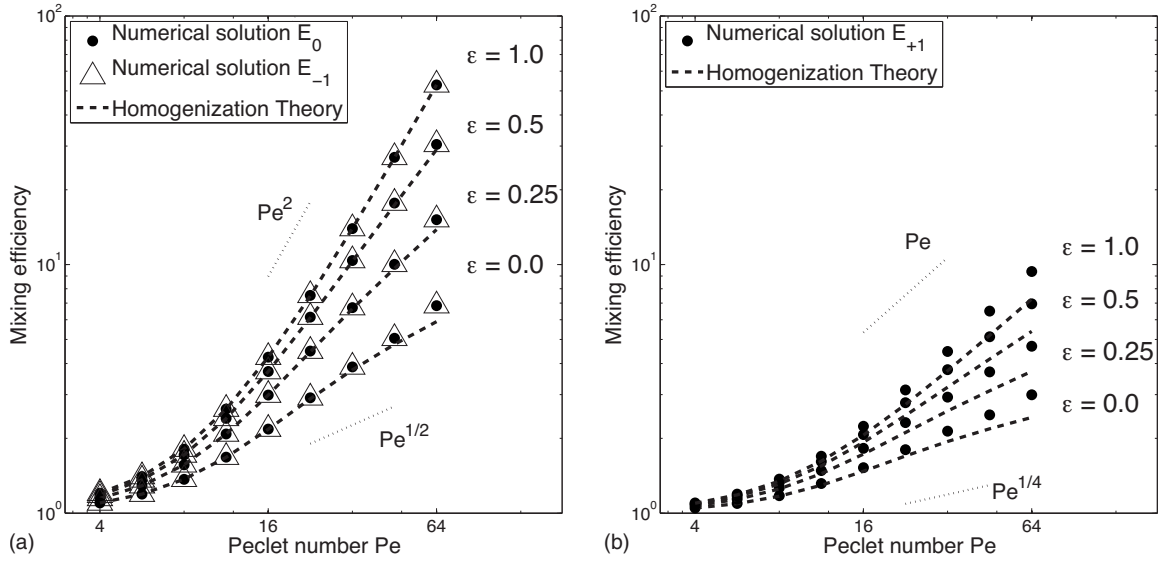

FIG. 3. Log-log plot of (left) unweighted mixing efficiency E_0 and macroscale- weighted mixing efficiency E_{-1} and (right) microscale-weighted mixing efficiency E_{+1} vs Péclet number Pe calculated for simulated Childress–Soward flows with monochromatic source $s(\boldsymbol{x})=\cos(x-y)/L$ with $\delta=\lambda/L=1/128$. Dashed lines plot the homogenization theory prediction for these mixing efficiencies (11a)–(11c). Dotted lines indicate predicted large Péclet number scalings for comparison.

$$\delta^{-1}\,\mathrm{Pe}^{1/2} \lesssim N. \tag{18}$$

We choose to explore the parameter ranges $1/128 \leq \delta \leq 1$ and $4 \leq \mathrm{Pe} \leq 64$. This will allow us to observe how the mixing measure behavior changes as the scales of the velocity and source field separate, and the relatively modest range of Pe is still wide enough (for these flows) to observe nontrivial scaling behavior [which actually seems to already be in the large Pe asymptotic regime for Pe=64 (Ref. 34)].

The only potentially significant numerical error in our simulations arises from the fact that, due to the smoothness of the source and the stirring field, the scalar variance (as well as the gradient and antigradient variances) approaches its asymptotic value very slowly so that it is necessary to end the simulation before the variance has reached its true $t \to \infty$ value. To minimize this source of error we evolved the scalar field until the variance changed by less than 0.01% over the diffusion time scale $\tau_{\mathrm{diff}}=1/\kappa k_s^2$ or longer.

First we explore the behavior of the mixing efficiencies when $\delta=\frac{1}{128}$, so that the source length scale is large compared to the stirring length scale, and homogenization theory can be expected to be relevant in describing the passive scalar dynamics. The equilibrium tracer variance, antigradient variance, and gradient variance thus obtained were used to calculate the multiscale mixing efficiencies (1), which are plotted against Péclet number in Fig. 3. In the case of a shear flow ($\epsilon=1.0$) both the macroscale-weighted mixing efficiency E_{-1} and unweighted mixing efficiency E_0 exhibit approximately Pe^2-scaling for large Péclet number. This scaling decreases with decreasing ϵ, corresponding to narrower channels and increased cross-channel blocking. For cellular flows ($\epsilon=0.0$) the E_{-1} and E_0 scale as $\mathrm{Pe}^{1/2}$. Also shown is the homogenization theory prediction (11a) and (11b), which, for the monochromatic source considered here, reduces to $1+\bar{K}(\hat{\boldsymbol{n}})$. Thus, the scalings of the mixing efficiencies for these Childress–Soward flows are in agreement with the high Péclet number scaling of the homogenized diffusivity $\bar{K}(\hat{\boldsymbol{n}})$ along channels, the most efficient transport direction (Fig. 2).

Also shown in Fig. 3 is the microscale-weighted mixing efficiency E_{+1}, which shows a shallower scaling with Pe than that of the other mixing efficiencies, namely, Pe for shear flows ($\epsilon=1.0$) and $\mathrm{Pe}^{1/4}$ for cellular flows ($\epsilon=0.0$). Superimposed on this figure is the homogenization theory prediction (11c), which, for monochromatic sources as here reduces to $(1+\bar{K}(\hat{\boldsymbol{n}}))^{1/2}$. Again, homogenization theory successfully captures the high Péclet number scaling of the microscale-weighted mixing efficiency, although the scaling is different from what a direct application of the homogenization theory result would imply. The fit is also not quite as good as for the larger scale mixing efficiencies E_0 and E_{-1}, presumably because the smaller-scale mixing efficiency E_{+1} is more sensitive to the finite scale separation between the source and stirring fields.

To probe the role played by scale separation in altering the scaling behavior of the mixing efficiency, we repeated the numerical experiments for more moderate scale separation, with values of δ varying between 1/12 and 1 (the case of no scale separation between source and stirring field). Our results are shown in Fig. 4. The smaller scale separation here allows one to explore higher Péclet numbers while still satisfying the resolution condition (18). Also shown are the homogenization theory predictions (11a)–(11c) in the homogenization limit $\delta=0$. In all cases, the mixing efficiency is suppressed below the homogenization theory prediction as scale separation is weakened ($\delta \to 1$). In the case of *no* scale

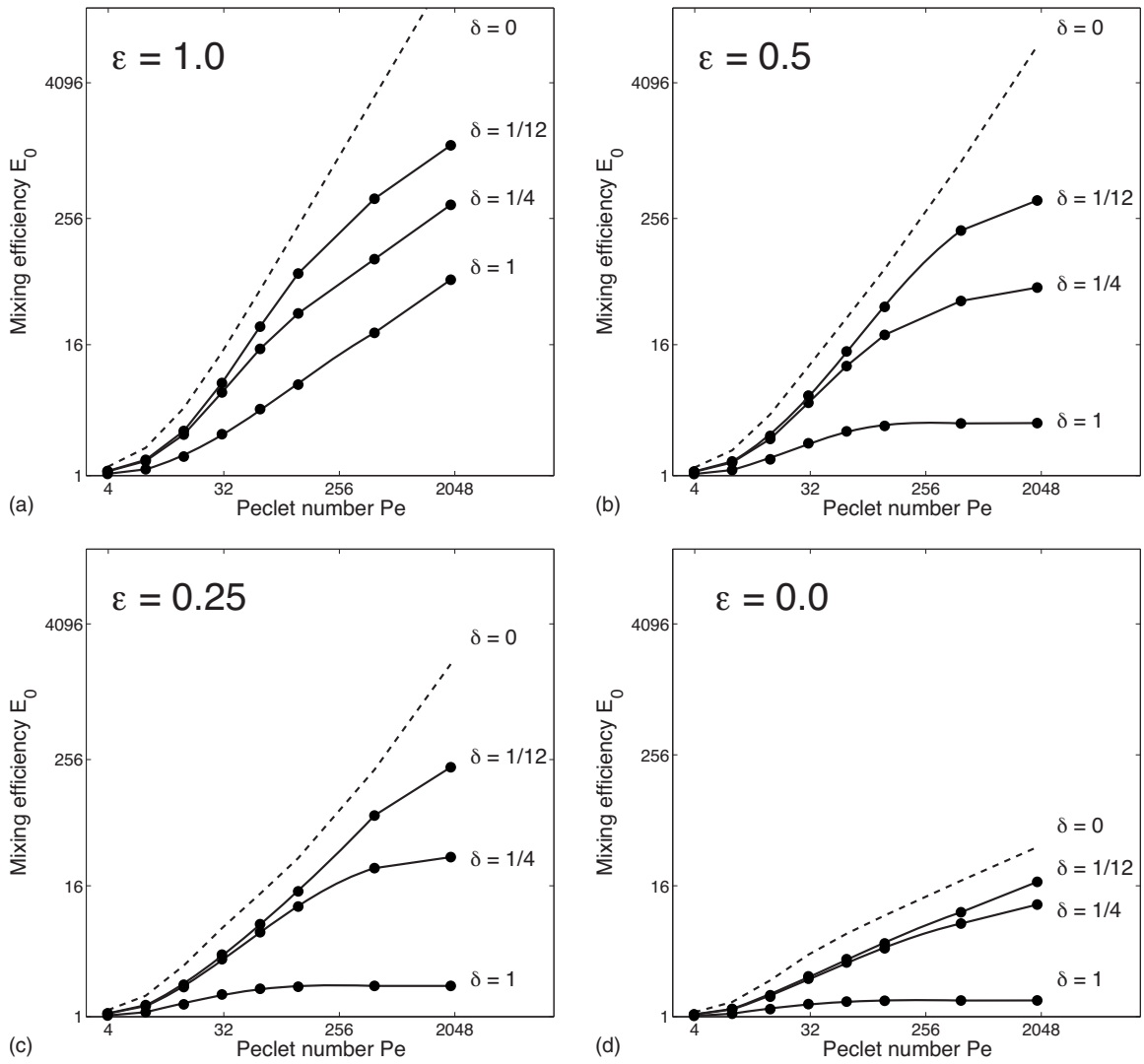

FIG. 4. Log-log plot of unweighted mixing efficiency vs Péclet number Pe for Childress–Soward flows with monochromatic source $s(\boldsymbol{x})=\cos(x-y)/L$. Each figure corresponds to one of the considered flow patterns (parametrized by ϵ), and in each figure, we examine different ratios of the scale separation parameter $\delta=\ell/L$ between the length scale of the stirring velocity field and the source. Dashed lines indicate the theoretical predictions (11a)–(11c) in the homogenization limit $\delta=0$.

separation, the mixing efficiency plateaus for $\epsilon<1$, remaining constant as Pe increases. This behavior is hardly a surprise: unlike chaotic advection, wherein a large-scale, time-varying velocity field can strongly mix a passive scalar field,[1] the time-independent laminar flows we consider are unable to generate the small scales necessary for efficient mixing unless the scale of the source is much larger than that of the stirring field, as shown in Fig. 5. We recall that homogenization theory is only expected to be valid in the limit[2,18]

$$\delta \ll 1, \mathrm{Pe}^{-1}. \tag{19}$$

This is consistent with the results in Fig. 3, which shows parameter ranges satisfying these conditions as well as agreement with the predictions of homogenization theory. Homogenization theory is shown by Lin *et al.*[23] to work well for the mixing of a source with a shear flow precisely when condition (19) is met, and fails to be relevant as soon as this condition is violated.

IV. CONCLUSIONS

We have examined the multiscale mixing efficiencies of Doering and Thiffeault[13] through the lens of homogenization theory by considering situations in which the length scale of the passive scalar source/sink field is large compared to the length scale of the stirring velocity field. For simplicity, we have considered periodic velocity fields, although the machinery of homogenization theory and our analysis can also be developed for velocity fields and source fields that are modeled as homogenous *random* functions (a more plausible model of real-world turbulence) provided the correlations in the flow are sufficiently short-range.[2,18,19,24–28] The required small parameter for the validity of homogenization theory would then be the ratio of the correlation length of the stirring velocity field to that of the source field.

We have derived theoretical expressions for the mixing efficiencies when the conditions for homogenization theory are satisfied, and showed that they imply that the mixing

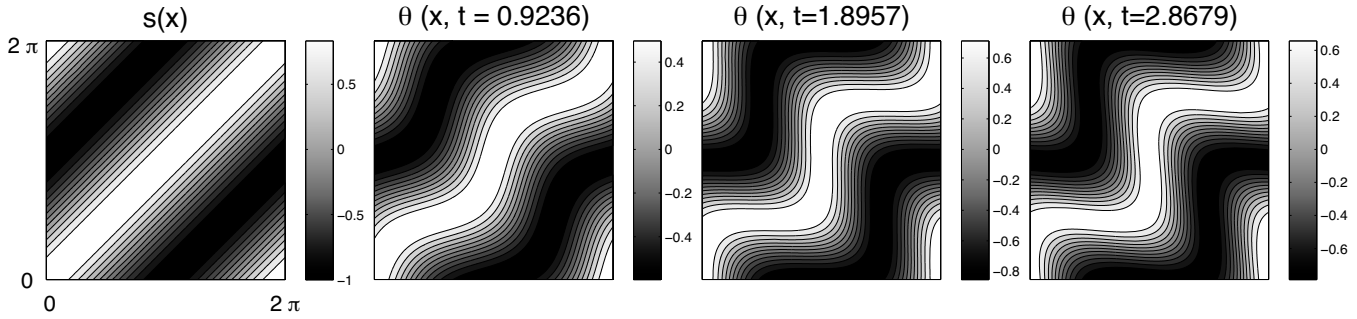

FIG. 5. Snapshots of source function $s(\boldsymbol{x})$ and scalar concentration $\theta(\boldsymbol{x},t)$ at various time-steps for a stirring shear flow with no scale separation ($\delta=1.0$ and $\epsilon=1.0$). The stirring field is unable to generate the small scales in the scalar concentration necessary for efficient mixing.

efficiencies should thereby scale in a similar way to the homogenized diffusivities at large Péclet numbers, provided the mixing efficiency does not weigh the small scales too much. We have examined how the small-scale fluctuations generated by the velocity field affect the mixing measures in ways that differ from the direct homogenization prediction, but can be reconciled with a more careful application of homogenization theory. Through numerical experiments with the Childress–Soward family of flows, we show how the homogenization predictions for the mixing measures deteriorate as the length scales of the stirring and force field approach each other, complementing the study of this phenomenon through shear flows in Lin *et al.*[23]

One consequence of our above considerations is that, when the source scale is large compared to the stirring scale, the flows which maximize or minimize mixing [as quantified by the multiscale mixing measures (1)] are the same as those which maximize or minimize turbulent transport, provided the flow is oriented appropriately with respect to the source-sink distributions. The issue of optimal mixing for the case when the source and velocity field have the same length scale of variation is explored in Refs. 9 and 38.

Finally we note an interesting practical implication of some of the results presented in this study. The usual advection-diffusion equation for a scalar field with an imposed slowly varying background gradient $\boldsymbol{\nabla}\bar{\theta}(\boldsymbol{x},t)$ can be written as

$$\frac{\partial\theta}{\partial t}+\mathcal{L}\theta=-\boldsymbol{v}(\boldsymbol{\xi},\tau)\cdot\boldsymbol{\nabla}\bar{\theta},\quad \mathcal{L}=\boldsymbol{v}(\boldsymbol{\xi},\tau)\cdot\boldsymbol{\nabla}-\kappa\Delta, \tag{20}$$

where $(\boldsymbol{\xi},\tau)$ and $(\boldsymbol{x},t)$ are the fast and slow space-time variables, respectively. By comparison with Eq. (5) it can be seen that Eq. (20) is equivalent to the evolution equation for a replenishing passive scalar field forced by the background gradient term $s(\boldsymbol{\xi},\tau;\boldsymbol{x},t)=-\boldsymbol{v}(\boldsymbol{\xi},\tau)\cdot\boldsymbol{\nabla}\bar{\theta}(\boldsymbol{x},t)$. This term takes the form of a rapidly varying source of scalar variance modulated by a slowly varying amplitude.

The multiscale mixing efficiencies for this particular source-flow combination are given by

$$\mathcal{E}_p(\boldsymbol{x},t)=\mathcal{D}_p(\boldsymbol{x},t)/\kappa, \tag{21}$$

where

$$\mathcal{D}_p(\boldsymbol{x},t)=\sqrt{\frac{\langle|\boldsymbol{\nabla}^{p-2}s|^2\rangle_{\boldsymbol{\xi},\tau}}{\langle|\boldsymbol{\nabla}^{p}\theta|^2\rangle_{\boldsymbol{\xi},\tau}}} \tag{22}$$

are the so-called *equivalent diffusivities* required to suppress, by diffusion alone, the scalar variances $\langle|\boldsymbol{\nabla}^p\theta|^2\rangle$ to the same values obtained in the presence of the stirring field $\boldsymbol{v}(\boldsymbol{x},t)$ and the molecular diffusivity κ.[15] [Note that the averages in Eq. (22) are taken over the fast space and time variables only.] In this sense, the $\mathcal{D}_p$ can be thought of as exact characterizations of the scalar dissipation by the subgrid-scale stirring field that can be calculated for any scale separation.

Following the arguments of Sec. II, it can be shown that, in the limit $\delta\to 0$, $\mathcal{D}_p$ takes the value of the enhanced diffusivity $\mathsf{D}=\kappa(\mathsf{I}+\overline{\mathsf{K}})$ projected onto the mean gradient direction $\boldsymbol{\nabla}\bar{\theta}/|\boldsymbol{\nabla}\bar{\theta}|$. Thus, the equivalent diffusivities reproduce the usual homogenization theory prediction in the limit of infinite scale separation, while at finite scale separations they will typically vary from this prediction. As such, they are potentially more flexible mixing diagnostics than the homogenized diffusivity, providing a physically meaningful quantification of mixing for passive scalar advection problems with finite scale separations while agreeing with the homogenization theory prediction in the $\delta\to 0$ limit. Thus, by comparing $\mathcal{D}_p$ with the effective diffusivity one obtains a measure for how well homogenization theory parametrizes subgrid-scale mixing for flows with finite scale separation between the stirring field and the mean scalar field. We will take up this topic in the context of temporally unsteady velocity fields in a future publication.

ACKNOWLEDGMENTS

This work has greatly benefitted from discussions with Banu Baydil, Roberto Camassa, Charlie Doering, Zhi Lin, Rich McLaughlin, and Igor Mezic, to whom we are most grateful. We are happy to acknowledge the support for this research from a National Science Foundation "Collaborations in Mathematical Geosciences" (Grant No. OCE-0620956).

APPENDIX: CALCULATION OF THE MICROSCALE-WEIGHTED MIXING EFFICIENCY IN THE LIMIT OF STRONG SCALE SEPARATION

The formal derivation of the effective diffusion equation in the presence of a source-sink distribution is presented in detail in Ref. 18. In the typical homogenization theory formulation, one seeks to obtain a description of the long-time, large-scale evolution of $\theta(\boldsymbol{x},t)$ by rescaling variables $\boldsymbol{x}\to\delta^{-1}\boldsymbol{x}$, $t\to\delta^{-2}t$, and then, in these new coordinates, distinguishing dynamics on small $(\boldsymbol{\xi}=\boldsymbol{x}/\delta, \tau=t/\delta^2)$ and large $(\boldsymbol{x},t)$ space and time scales, separately, so that[2]

$$\nabla\to\nabla_{\boldsymbol{x}}+\delta^{-1}\nabla_{\boldsymbol{\xi}},\quad \partial_t\to\partial_t+\delta^{-2}\partial_\tau. \tag{A1}$$

Note that in the current setup, the small spatial scale corresponds to the scale of variation of the stirring field, while the large scale corresponds to the scale of variation of the source field. One then seeks a solution to the advection-diffusion equation for the passive tracer via a perturbative expansion in the small parameter δ,

$$\theta^{(\delta)}(\boldsymbol{x},t)=\overset{(0)}{\theta}(\boldsymbol{\xi},\tau;\boldsymbol{x},t)+\delta\overset{(1)}{\theta}(\boldsymbol{\xi},\tau;\boldsymbol{x},t)+\delta^2\overset{(2)}{\theta}\times(\boldsymbol{\xi},\tau;\boldsymbol{x},t)\cdots|_{\boldsymbol{\xi}=\delta^{-1}\boldsymbol{x},\tau=\delta^{-2}t}. \tag{A2}$$

To calculate the microscale-weighted mixing efficiency E_{+1} we require the gradient of the stirred tracer field; from Eqs. (A1) and (A2) this is

$$\nabla\theta^{(\delta)}=(\nabla_{\boldsymbol{x}}\overset{(0)}{\theta}+\nabla_{\boldsymbol{\xi}}\overset{(1)}{\theta})|_{\boldsymbol{\xi}=\boldsymbol{x}/\delta,\tau=t/\delta^2}+O(\delta). \tag{A3}$$

Proceeding with the usual homogenization theory development, we substitute the expansions (A1) and (A2) into the advection diffusion equation and solve at each order in δ, finding[2]

$$\overset{(0)}{\theta}(\boldsymbol{\xi},\tau;\boldsymbol{x},t)=\bar{\theta}(\boldsymbol{x},t), \tag{A4}$$

$$\overset{(1)}{\theta}(\boldsymbol{\xi},\tau;\boldsymbol{x},t)=\boldsymbol{\chi}(\boldsymbol{\xi},\tau)\cdot\nabla_{\boldsymbol{x}}\bar{\theta}(\boldsymbol{x},t)+\bar{\theta}_1(\boldsymbol{x},t). \tag{A5}$$

The zeroth order solution can be interpreted as stating that the large-scale variations of the passive scalar density are dominant, and subsequent calculations at the second order of the asymptotic hierarchy show that $\bar{\theta}$ evolves according to the effective diffusion Eq. (8) [dropping the $O(\delta)$ error terms]. The first-order solution comprises both the leading order *small-scale* response of the passive scalar field and a higher order correction $\bar{\theta}_1$ to the large-scale variation, the latter of which plays no essential role to our final results. The small-scale component is expressed in terms of a vector field $\boldsymbol{\chi}(\boldsymbol{\xi},\tau)$ that is the unique, periodic, mean-zero solution of the auxiliary cell problem

$$(\partial_\tau+\boldsymbol{v}(\xi,\tau)\cdot\nabla_{\boldsymbol{\xi}}-\kappa\Delta_{\boldsymbol{\xi}})\boldsymbol{\chi}(\boldsymbol{\xi},\tau)=-\boldsymbol{v}(\boldsymbol{\xi},\tau), \tag{A6}$$

and determines the enhanced diffusivity tensor via the formula

$$\bar{\mathsf{K}}_{ij}=\langle\nabla_{\boldsymbol{\xi}}\chi_i\cdot\nabla_{\boldsymbol{\xi}}\chi_j\rangle. \tag{A7}$$

Substituting expressions (A4) and (A5) into the expansion (A3) yields

$$\langle|\nabla\theta|^2\rangle_{\boldsymbol{\xi},\tau}=\sum_{i,j=1}^{d}\left(\delta_{ij}+\left\langle\frac{\partial\chi_i}{\partial\xi_j}+\frac{\partial\chi_i}{\partial\xi_j}\right\rangle_{\boldsymbol{\xi},\tau}+\langle\nabla_{\boldsymbol{\xi}}\chi_i\cdot\nabla_{\boldsymbol{\xi}}\chi_j\rangle_{\boldsymbol{\xi},\tau}\right)\frac{\partial\bar{\theta}}{\partial x_i}\frac{\partial\bar{\theta}}{\partial x_j}+O(\delta), \tag{A8}$$

where $\langle\cdot\rangle_{\boldsymbol{\xi},\tau}$ represents averaging over small-scale variables only. From the periodic boundary conditions on $\boldsymbol{\xi}$ and τ, the second term in brackets vanishes; using expression (A7) then gives the gradient variance in the $\delta\to0$ limit as

$$G(\boldsymbol{x},t)=\sum_{i,j=1}^{d}(\delta_{ij}+\bar{K}_{ij})\frac{\partial\bar{\theta}}{\partial x_i}\frac{\partial\bar{\theta}}{\partial x_j}. \tag{A9}$$

A direct estimation of the passive scalar gradient as the gradient of $\bar{\theta}$ would neglect the $\bar{K}_{ij}$ term, which arises from the fact that the small-scale gradient of the formally subdominant first-order term contributes on equal terms to the large-scale gradient of the leading order term.

Fourier transforming Eq. (A9) with respect to the slowly varying spatial coordinate $\boldsymbol{x}$ and substituting in the equilibrium solution (10) gives

$$\hat{G}_{\boldsymbol{k}}=\frac{|\hat{s}_{\boldsymbol{k}}|^2}{\kappa^2(k^2+\bar{K}_{ij}k_ik_j)}, \tag{A10}$$

so that the microscale-weighted mixing efficiency becomes, in the limit $\delta\to0$,

$$E_{+1}^2=\frac{\langle|\nabla\theta_0|^2\rangle}{\langle|\nabla\theta|^2\rangle}=\frac{\Sigma_{\boldsymbol{k}}|\hat{s}_{\boldsymbol{k}}|^2/k^2}{\Sigma_{\boldsymbol{k}}|\hat{s}_{\boldsymbol{k}}|^2\Big/\left(k^2+\Sigma_{i,j=1}^{d}\bar{K}_{ij}k_ik_j\right)}. \tag{A11}$$

[1] J. M. Ottino, "Mixing, chaotic advection, and turbulence," Annu. Rev. Fluid Mech. **22**, 207 (1990).
[2] A. J. Majda and P. R. Kramer, "Simplified models of turbulent diffusion: Theory, numerical modelling, and physical phenomena," Phys. Rep. **314**, 237 (1999).
[3] Z. Warhaft, "Passive scalars in turbulent flows," Annu. Rev. Fluid Mech. **32**, 203 (2000).
[4] B. I. Shraiman and E. D. Siggia, "Scalar turbulence," Nature (London) **405**, 639 (2000).
[5] B. Sawford, "Turbulent relative dispersion," Annu. Rev. Fluid Mech. **33**, 289 (2001).
[6] G. Falkovich, K. Gawedzki, and M. Vergassola, "Particles and fields in turbulence," Rev. Mod. Phys. **73**, 913 (2001).
[7] H. Aref, "The development of chaotic advection," Phys. Fluids **14**, 1315 (2002).
[8] S. Wiggins and J. M. Ottino, "Foundations of chaotic advection," Philos. Trans. R. Soc. London, Ser. A **362**, 937 (2004).
[9] G. Mathew, I. Mezic, S. Grivopoulos, U. Vaidya, and L. Petzold, "Optimal control of mixing in Stokes fluid flow," J. Fluid Mech. **580**, 261 (2007).
[10] M. H. England and E. Maier-Reimer, "Using chemical tracers to assess ocean models," Rev. Geophys. **39**, 29, doi:10.1029/1998RG000043 (2001).
[11] A. Mahadevan and J. W. Campbell, "Biogeochemical patchiness at the sea surface," Geophys. Res. Lett. **29**, 1926, doi:10.1029/2001GL014116 (2002).
[12] J. Marshall, E. Shuckburgh, H. Jones, and C. Hill, "Estimates and implications of surface eddy diffusivity in the Southern Ocean from tracer transport," J. Phys. Oceanogr. **36**, 1806 (2006).
[13] C. R. Doering and J.-L. Thiffeault, "Multiscale mixing efficiencies for steady sources," Phys. Rev. E **74**, 025301 (2006).
[14] G. Mathew, I. Mezić, and L. Petzold, "A multiscale measure for mixing," Physica D **211**, 23 (2005).

[15]J.-L. Thiffeault, C. R. Doering, and J. D. Gibbon, "A bound on mixing efficiency for the advection-diffusion equation," J. Fluid Mech. **521**, 105 (2004).
[16]T. A. Shaw, J.-L. Thiffeault, and C. R. Doering, "Stirring up trouble: Multi-scale mixing measures for steady scalar sources," Physica D **231**, 143 (2007).
[17]T. Okabe, B. Eckhardt, J.-L. Thiffeault, and C. R. Doering, "Mixing effectiveness depends on the source-sink structure: Simulation results," J. Stat. Mech.: Theory Exp. **2008**, P07018 (2008).
[18]P. R. Kramer and S. R. Keating, "Homogenization theory for a replenishing passive scalar field," Chin. Ann. Math., Ser. B **30**, 631 (2009).
[19]G. C. Papanicolaou and S. R. S. Varadhan, "Boundary value problems with rapidly oscillating random coefficients," in *Random Fields: Rigorous Results in Statistical Mechanics and Quantum Field Theory*, Colloquia Mathematica Societatis János Bolyai Vol. 2, edited by J. Fritz, J. L. Lebowitz, and D. Szasz (North Holland-Elsevier Science, Amsterdam, 1979), pp. 835–873.
[20]D. Cioranescu and P. Donato, *An Introduction to Homogenization* (Oxford University Press, New York, 1999), Chaps. 8, 9, and 11.
[21]A. Bensoussan, J.-L. Lions, and G. C. Papanicolaou, *Asymptotic Analysis for Periodic Structures*, Studies in Mathematics and Its Applications Vol. 5 (North Holland-Elsevier Science, Amsterdam, 1978), Chaps. 1 and 2.
[22]V. V. Jikov, S. M. Kozlov, and O. A. Oleinik, *Homogenization of Differential Operators and Integral Functions* (Springer-Verlag, Berlin, 1994), Chap. 2, pp. 55–85.
[23]Z. Lin, K. Bod'ová, and C. R. Doering, "Models and measures of mixing and effective diffusion," Discrete Contin. Dyn. Syst., Ser. B **28**, 259 (2010).
[24]M. Avellaneda and M. Vergassola, "Stieltjes integral representation and effective diffusivities in time-dependent flows," Phys. Rev. E **52**, 3249 (1995).
[25]M. Avellaneda and A. J. Majda, "Stieltjes integral representation and effective diffusivity bounds for turbulent transport," Phys. Rev. Lett. **62**, 753 (1989).
[26]A. Fannjiang and G. C. Papanicolaou, "Diffusion in turbulence," Probab. Theory Relat. Fields **105**, 279 (1996).
[27]K. Oelschläger, "Homogenization of a diffusion process in a divergence-free random field," Ann. Probab. **16**, 1084 (1988).
[28]S. Olla, "Homogenization of diffusion processes in random fields," Lecture Notes at École Polytechnique, 1994.
[29]M. Avellaneda and A. J. Majda, "An integral representation and bounds on the effective diffusivity in passive advection by laminar and turbulent flows," Commun. Math. Phys. **138**, 339 (1991).
[30]A. Fannjiang and G. Papanicolaou, "Convection-enhanced diffusion for periodic flows," SIAM J. Appl. Math. **54**, 333 (1994).
[31]S. Heinze, "Diffusion-advection in cellular flows with large Péclet numbers," Arch. Ration. Mech. Anal. **168**, 329 (2003).
[32]L. Biferale, A. Crisanti, M. Vergassola, and A. Vulpiani, "Eddy diffusivities in scalar transport," Phys. Fluids **7**, 2725 (1995).
[33]A. Crisanti and A. Vulpiani, "On the effects of noise and drift in diffusion in fluids," J. Stat. Phys. **70**, 197 (1993).
[34]A. J. Majda and R. M. McLaughlin, "The effect of mean flows on enhanced diffusivity in transport by incompressible periodic velocity fields," Stud. Appl. Math. **89**, 245 (1993).
[35]S. Childress and A. M. Soward, "Scalar transport and alpha-effect for a family of cat's-eye flows," J. Fluid Mech. **205**, 99 (1989).
[36]A. Crisanti, M. Falcioni, G. Paladin, and A. Vulpani, "Anisotropic diffusion in fluids with steady periodic velocity fields," J. Phys. A **23**, 3307 (1990).
[37]G. I. Taylor, "Dispersion of soluble matter in solvent flowing slowly through a tube," Proc. R. Soc. London, Ser. A **219**, 186 (1953).
[38]J.-L. Thiffeault and G. A. Pavliotis, "Optimizing the source distribution in fluid mixing," Physica D **237**, 918 (2008).